

2002

NASA FACULTY FELLOWSHIP PROGRAM

**MARSHALL SPACE FLIGHT CENTER
THE UNIVERSITY OF ALABAMA**

THERMO-MECHANICAL PROCESSING IN FRICTION STIR WELDS

Prepared by:	Judy Schneider, Ph.D.
Academic Rank:	Assistant Professor
Institution and Department:	Mississippi State University Department of Mechanical Engineering
NASA/MSFC Directorate:	Engineering Materials, Processes and Manufacturing (ED 30)
MSFC Colleague:	Arthur C. Nunes, Jr., Ph.D.

Abstract

Friction stir welding is a solid-phase joining, or welding process that was invented in 1991 at The Welding Institute (TWI) [1]. The process is potentially capable of joining a wide variety of aluminum alloys that are traditionally difficult to fusion weld. The friction stir welding (FSW) process produces welds by moving a non-consumable rotating pin tool along a seam between work pieces that are firmly clamped to an anvil. At the start of the process, the rotating pin is plunged into the material to a pre-determined load. The required heat is produced by a combination of frictional and deformation heating. The shape of the tool shoulder and supporting anvil promotes a high hydrostatic pressure along the joint line as the tool shears and literally stirs the metal together. To produce a defect free weld, process variables (RPM, transverse speed, and downward force) and tool pin design must be chosen carefully. An accurate model of the material flow during the process is necessary to guide process variable selection.

At MSFC a plastic slip line model [2] of the process has been synthesized based on macroscopic images of the resulting weld material. Although this model appears to have captured the main features of the process, material specific interactions are not understood. The objective of the present research was to develop a basic understanding of the evolution of the microstructure to be able to relate it to the deformation process variables of strain, strain rate, and temperature.

Background

A striking feature of the FSW microstructure is a central nugget, shown in Figure 1. The macroscopic features are typically described as an outer heat affected zone (HAZ), an inner thermo-mechanically affected zone (TMAZ), and a central nugget of fine, equiaxed grains. Under a light microscope, this central nugget displays layers of varying thickness, like onion rings [3]. The variations and spiral development are reported to vary with the ratio of weld velocity (V) to pin rotation [3], and can also be observed in the transverse section of the weld shown in Figure 2.

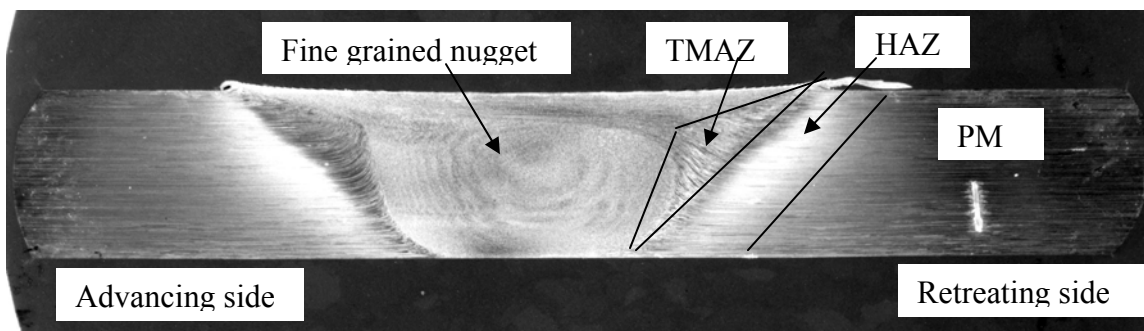


Fig. 1. Optical image of FSW cross-section.

Microscopically the grain morphology shows a transition from the elongated, rolled grains of the parent material (PM) (80 to 100 μm dia. in plane view), to an equiaxed grain of 0.5-10 μm within the nugget. Figure 3 shows this delineation between the TMAZ nugget to be quite sharp. The deformation of the base metal in the TMAZ manifests itself as bending of the grains in the plane of the metallographic section.

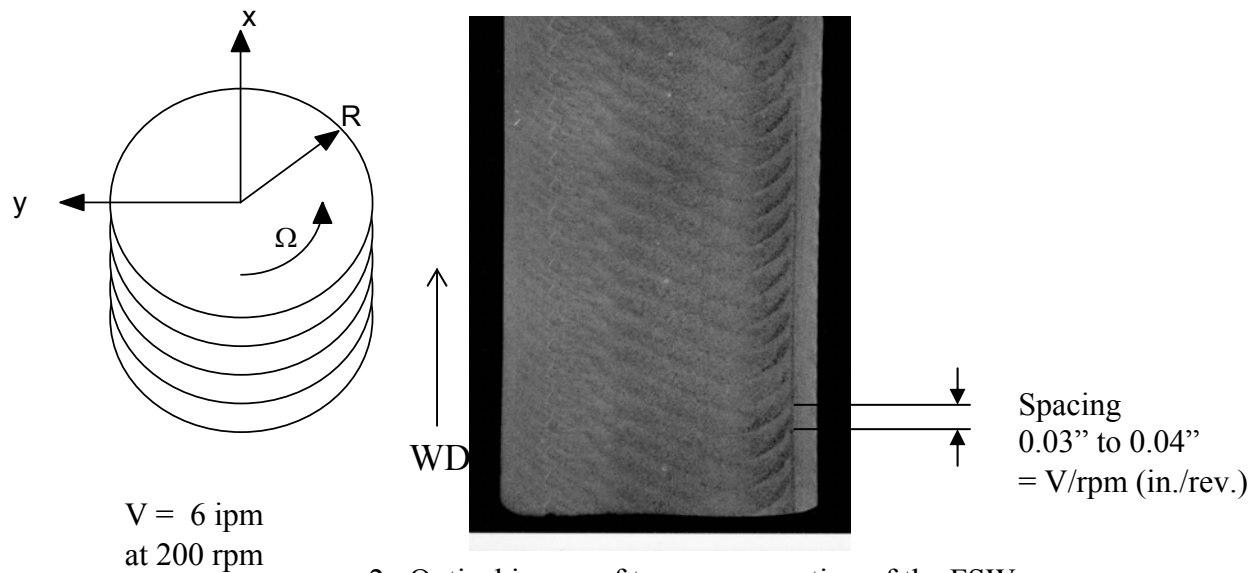


Fig. 2. Optical image of transverse section of the FSW.

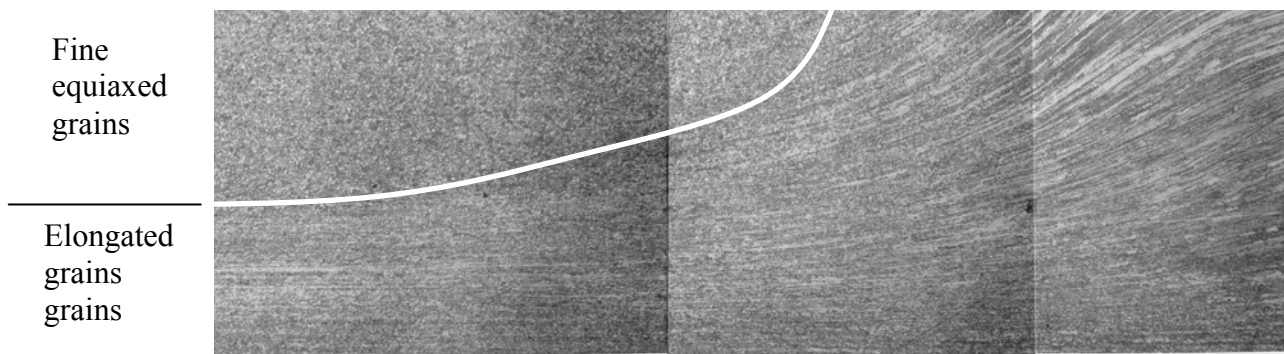


Fig. 3. Optical image of transition from elongated grains (right) into the fine grained, retreating side of the nugget (shoulder side on bottom).

Several FSW flow visualization studies have been reported in the literature using either dissimilar materials or tracer techniques. Li et. al., [4, 5] described patterns observed on metallographic cross sections in FWS made between dissimilar Al alloys and between Al alloys and Cu. Differential etching of the dissimilar materials revealed material flow patterns, described as a chaotic-dynamic mixing.

Colligan [6] studied the material flow using embedded steel spheres placed along the weld centerline prior to welding. This approach allowed single points to be followed in the weld process as interpreted by post weld xray inspection. Colligan reported that material is stirred only in the upper portion of the weld and that in the rest of the weld materials is simply extruded around the pin. However, a concern has been whether the 0.015" dia. steel tracer spheres used in his study, would flow in the same way as the Al alloy during welding. Also, no information on shear zone behavior can be obtained.

Seidel and Reynolds [7] utilized a marker insertion technique to investigate the shearing around the tool pin. The flow path was reconstructed using a serial sectioning technique to produce three-dimensional plots of the deformed marker. The flow visualization studies all indicate the flow path or deformation process in a FSW is complicated and may even consist of several paths. It is possible that the confinement of the shoulder and anvil set up flow at the plate surfaces different from the flow established by the weld pin geometry.

To explain the results of the flow visualization studies, a wiping model of the material flow in FWS has been proposed that is similar to an orthogonal metal cutting model [2]. In this

model a rapidly rotating cylinder is super positioned within a slowly rotating ring vortex, and a uniform translation flow generates a ‘wiping’ flow that appears to model the plastic flow around the pin-tool. This model predicts almost instantaneous strain increments. A marker experiment was conducted to investigate the magnitude of the shear zone. Tungsten was selected as a marker due to its high melting temperature, and brittle mechanical behavior. Temperature measurements in Al alloys [8] along with analytical predictions indicate a temperature of 450° C in the welding of Al alloys. This corresponds to 0.2 times the absolute melting temperature of tungsten, at which no appreciate change in mechanical properties is expected. Reported shear strength of drawn tungsten wire is 58 ksi [9].

Experimental procedure

The material used in this study was an Al-Li-Cu alloy. The plate had a thickness of 8.2 mm (0.323”) and was welded along the plate rolling direction. A thin 0.0025” diameter wire was placed transversely along the center of the plates. The plates were then tack welded together prior to clamping in the vertical welding tool (VWT). An initial pass was made to join the plates at the surface prior to the full penetration FSW. Tungsten wire placement was verified prior to the start of the full penetration FSW process. After welding the plates were x-ray inspected in the transverse (Figure 5) and normal (Figure 6) directions to the FSW. Serial sectioning was used to verify wire segment spacing. Keller’s regent was used to reveal the grain structure in metallographic samples. The wire marker tends to agree with Colligan’s research [6], but illustrates the severe shearing zone the material enters during FSW.

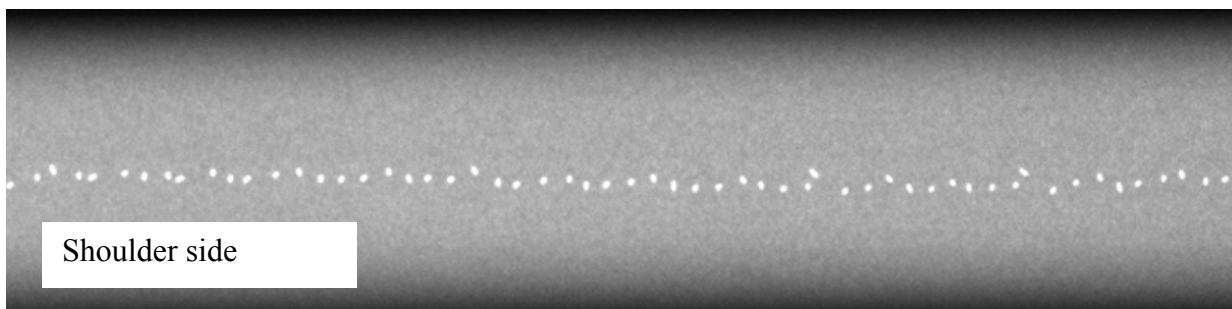


Fig. 5. Transverse x-ray of FSW



Fig. 6. Normal x-ray of FSW. Tungsten wire segments are 0.025” in length and are spaced 0.020 to 0.028” apart.

Discussion

The material being welded is sheared under a compressive load to large strains associated with plastic flow. The shear zone is confined, or hydrostatically loaded, by the surrounding parent material, the anvil and the tool shoulder. Conservation of volume in this process means that there will be local changes in displacement and velocity, which result in gradients of strain and strain rate. The effects of pressure can alter the rate controlling mechanisms for deformation since at elevated temperatures; diffusion will be slowed due to limited vacancies, making the glide of dislocations more favorable.

The range of distinct grain morphology and sizes observed in the FSW zones is an indication of the strain, strain rate, and temperature conditions the material has undergone in the TMAZ. The parent material is characterized by pancake shaped grains, typical of that resulting from cold rolling. The initial grains are in the range of 60 to 80 microns in diameter and 0.5 to 10 microns in thickness. In the weld nugget fine, equiaxed, high grain boundary angles of 15-20° are observed [10-13].

Most commonly, the mechanism of the grain size variations is reported to be recrystallization with subsequent grain growth. One researcher reported the refined grain size to be stable and unaffected by subsequent heat treatments up to 65 h at 150 °C under static conditions [12]. Another researcher compared the grain boundary orientation of the nugget before and after a post weld heat treatment at 500 C for 10 s and concluded that the orientation in the nugget reflected that of a dynamically, not statically, recrystallized grain boundary angle [13]. Murr [14] has reported seeing spiral dislocations present in TEM studies, indicative of dislocation climb, and suggestive of a continuous recrystallization process.

The constant hardness profile reported for pure Al alloy (1100) [14] can be explained by self-compensating strengthening mechanisms and used to determine a dislocation density profile corresponding to the grain morphology. Plates of Al alloys are usually cold rolled which strengthens the plate by increasing dislocation density (ρ) or strain hardening (eqn. 1). As the grains undergo recrystallization, the annihilation of strain induced dislocations result in the formation of smaller, equiaxed grains. An increase in strengthening is noted as the grain size (d) decreases (eqn. 2). The material threshold stress is given as σ_o , flow stress is given as σ_{ys} and k values are the material constants.

$$\sigma_{ys} = \sigma_o + k_1 (\rho)^{0.5} \quad \text{eqn. 1}$$

$$\sigma_{ys} = \sigma_o + k_2 / (d)^{0.5} \quad \text{eqn. 2}$$

Using material constants from the literature [15], a constant hardness can be maintained assuming a dislocation density of 10^{12} in the 100 μm parent material to a dislocation density of 10^8 in the recrystallized grains of 10 nm. A dislocation density of 10^{12} was selected as representative of a strained microstructure, while 10^8 was selected as representative of a unstrained microstructure.

Conclusions

Very fine, recrystallized grains are observed in the weld nugget toward the anvil side of the weld, on the retreating side as shown in Figure 7. This suggests that TMAZ processing associated with the FSW results in an appropriate level of strain for the temperature profile that results in a high level of grain refinement. The effects of the heat input may subsequently cause the grains to grow. Conversely, this distribution of fine grains may suggest that different flow paths are subjected to different strain accumulations which may affect the final recrystallized

grain size under the imposed temperature. Data shown in Figure 8 illustrate the tradeoffs in total strain vs recrystallization temperatures [16].

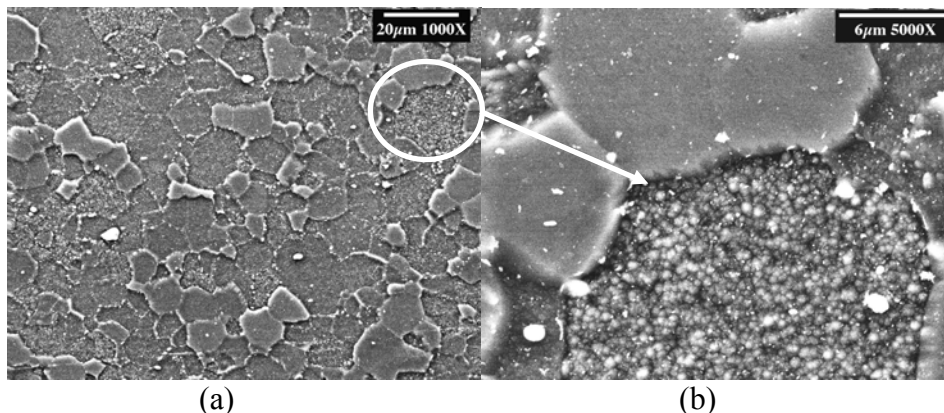


Fig. 7. a) SEM-SE image of recrystallized region of FWS,
b) Closeup image of recrystallized region in Figure 7a.

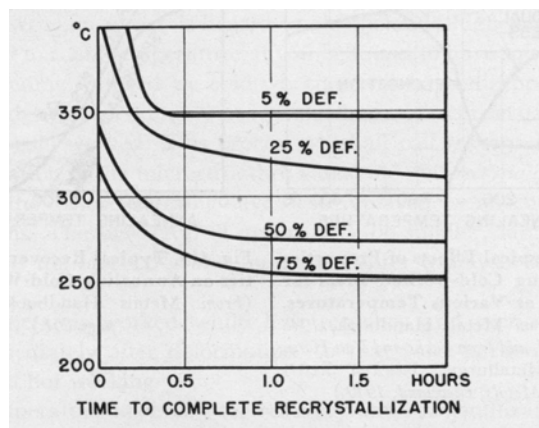


Fig. 8. Effect of strain on recrystallization temperature [16].

References

- 1 Thomas, W.M., et. al., 1991. *Friction Stir Butt Welding*, U.S. Patent No. 5,460,317.
- 2 Nunes, A.C., Jr., "Wiping Metal Transfer in Friction Stir Welding", TMS Annual Meeting, New Orleans, LA, 2001.
- 3 Krishnan, K.N., *Mat. Sci. & Engr. A*, 327 (2002), 246-251.
- 4 Li, Y., Murr, L.E., McClure, J.C., *Scripta Mater.*, Vol. 40, No. 9, (1999) 1041-1046.
- 5 Li, Y., Murr, L.E., McClure, J.C., *Mat. Sci. & Engr.*, A271 (1999) 213-223.
- 6 Colligan, K., *Welding Research* (1999) 229s-237s.
- 7 Seidel, T.U., Reynolds, A.P., *Met. & Mat. Trans. A*, 32A (2001), p. 2879-2884.
- 8 Tang, W., Guo X., McClure, J.C., Murr, L.E., *J. Mat. Proc. & Mfgt. Sci.*, (1998), p. 163-172.
- 9 Materials Information Website, <http://www.matweb.com>.
- 10 Mishra, R.S., Mahoney, M.W., McFadden, S.X., Mara, N.A., Mukherjee, A.K., *Scripta mater.*, 42 (2000) 13-168.
- 11 Murr, L.E., Liu, G., McClure, J.C., *J. Mat. Sci. Letters*, 16 (1997) 1801-1803.
- 12 Jata, K.V., Semiatin, S.L. *Scripta mater.*, 43, (2000) 743-740.
- 13 Sato, Y.S., Kokawa, H., Ikeda, K., Enomoto, M., Jogan, S., Hashimoto, T., *Met. & Mat. Trans. A*, 32A, (2001) 941-948.
- 14 Murr, L.E., Li, G., McClure, J.C., *J. Mat. Sc. Letters*, 16 (1997) p. 1801-1803.
- 15 Barlow, et. al., *Act. metal.*, 2002.
- 16 Hultgren, R., *Fundamentals of Physical Metallurgy*, 1952, p. 158.